

Resource Management and Circuit Scheduling for Distributed Quantum Computing Interconnect Networks

Sima Bahrani*, Romerson D. Oliveira, Juan Marcelo Parra-Ullauri, Rui Wang[†], and Dimitra Simeonidou
*High Performance Networks Research Group, School of Electrical, Electronic, and Mechanical Engineering,
 University of Bristol, Bristol, UK*

E-mail: *sima.bahrani@bristol.ac.uk, [†]rui.wang@bristol.ac.uk

Abstract—Distributed quantum computing (DQC) has emerged as a promising approach to overcome the scalability limitations of monolithic quantum processors in terms of computing capability. However, realising the full potential of DQC requires effective resource management and circuit scheduling. This involves efficiently assigning each circuit to an optimal subset of quantum processing units (QPUs), based on factors such as their computational power and connectivity. In heterogeneous DQC networks with arbitrary topologies and non-identical QPUs, this becomes a complex challenge. This paper addresses resource management in such settings, with a focus on computing resource allocation in a quantum data center. We propose circuit scheduling and resource allocation algorithms that combine heuristic methods with a Mixed-Integer Linear Programming (MILP) formulation. Our MILP model accounts for infidelities arising from inter-QPU communication. The algorithms consider key factors including network topology, QPU characteristics, and quantum circuit structure to make efficient scheduling and allocation decisions. Simulation results demonstrate that our approach significantly improves circuit execution time and resource utilisation—measured by makespan, throughput, and QPU usage—while also reducing inter-QPU communication, compared to a baseline random allocation strategy. This work provides valuable insights into resource management strategies for scalable and heterogeneous DQC systems.

I. INTRODUCTION

Quantum computing has gained attention as a solution for tackling intractable problems, due to its capacity to solve them significantly faster than traditional computers. In recent years, there have been notable advancements in quantum hardware and control systems, leading to the development of noisy intermediate-scale quantum processing units (QPUs). However, despite these efforts, current quantum processors still remain limited in their computational power. In this context, distributed quantum computing (DQC) can offer a substantial benefit in scaling up quantum computing beyond the constraints of monolithic systems [1]–[4].

Distributed quantum computing aims to harness the collective power of multiple interconnected quantum processors, enabling the execution of larger and more complex quantum algorithms. In DQC, quantum algorithms are partitioned and executed across a network of quantum processors, which are interconnected through both quantum and classical communication channels. By distributing the computational workload

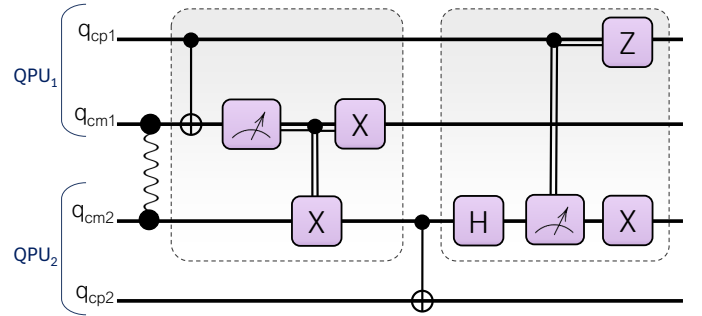


Fig. 1: Circuit diagram of remote CNOT gate performed between two QPUs.

among multiple quantum nodes, this approach facilitates the development of scalable quantum computing systems that can surpass the limitations imposed by individual quantum processors.

Distributed quantum computing is expected to progress through stages of increasing scale and heterogeneity [3]. This progression spans from the integration of multiple quantum processors within a single large quantum computer to the establishment of interconnected quantum processors across various quantum data centres. This work focuses on DQC within a single quantum data centre, where multiple quantum computers are interconnected via short-to-medium range links. A quantum data centre, in this context, refers to a facility housing quantum computers and the infrastructure for their operation and maintenance.

One of the fundamental requirements for DQC is the ability to perform quantum operations between distant qubits located on separate QPUs. Throughout this paper, we refer to such operations as *remote gates*. Most approaches proposed in the literature for realising remote gates rely on three key components: remote entanglement generation, local quantum operations on individual QPUs, and classical communication [1], [6]. As an illustrative example, Figure 1 shows the circuit diagram for implementing a controlled-NOT (CNOT) gate based on this approach between two *computing qubits*, denoted by q_{cp1} and q_{cp2} , belonging to separate QPUs (QPU₁ and QPU₂). The initial step in this method involves generating entanglement between two dedicated *communication qubits*,

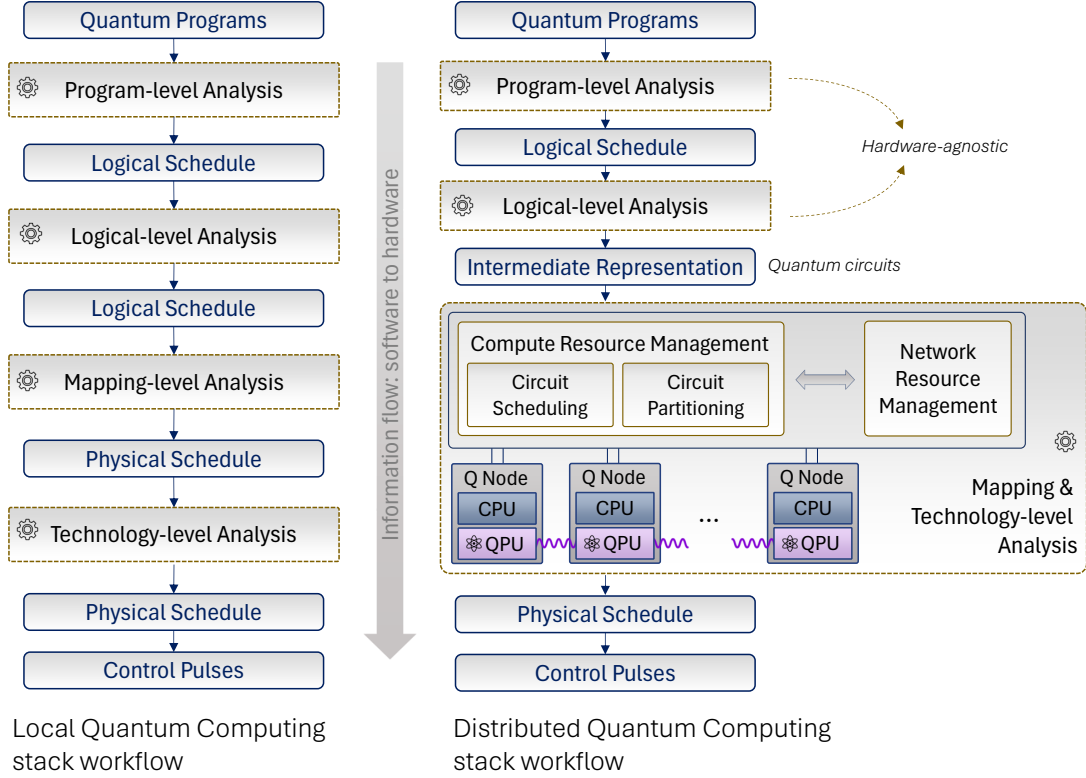


Fig. 2: Workflow of the quantum stack for both local and distributed quantum computing. A layered-oriented approach for compilation tools that bridge quantum algorithms with quantum devices. The stack workflow for local quantum computing, depicted on the left side of the figure, is based on [5].

denoted by q_{cm1} and q_{cm2} in Fig. 1, which facilitate the quantum communication between the QPUs. As depicted in the figure, the X operation on QPU₂ and the Z operation on QPU₁ are conditioned on the measurement outcome transmitted classically from the other QPU. The same approach can be extended to implement any controlled-unitary gate.

The integration of quantum networking, classical networking, and quantum computation within a DQC interconnect network requires efficient orchestration of various components and tasks. A critical element in this orchestration is quantum compilation, which translates a high-level description of a quantum program into a set of instructions to be applied to the physical hardware [5], [7]. This translation is performed through several layers of subroutines forming a compilation stack, as depicted in Fig. 2 [5]. In the context of DQC, additional tasks must be executed for an intermediate representation of the quantum program, which we refer to in this work as the *Quantum Circuit* (QCirc) (Fig. 2). These tasks involve various aspects of resource management, encompassing both network and compute resources. Compute resources primarily refer to the computing qubits embedded in QPUs, while communication resources include communication qubits and network components such as optical switches.

In this work, we assume that network and compute resource management are handled independently—a separation that enhances scalability and modularity, both of which are

essential in the complex DQC ecosystem. This assumption is consistent with the DQC architecture described in [3]. Within this framework, we assume the network can reliably establish entanglement links as needed to support remote operations between QPUs, and that network resource management can allocate the required resources, including communication qubits, on demand. As a result, our focus in this work is limited to compute resource management.

In the framework considered in this work, compute resource management is organised into two stages: *circuit scheduling* and *circuit partitioning*. Circuit scheduling manages the queue of QCircs, determines the set of QPUs allocated to each QCirc, and addresses the QCirc-to-QPU mapping problem in the presence of multiple concurrent user requests. Circuit partitioning then optimises the division of each QCirc into smaller sub-circuits, taking into account the number of partitions, the specific QPUs assigned during scheduling, and the structure of the circuit.

This paper focuses on the circuit scheduling problem in a quantum data centre environment within the DQC framework described above. Task scheduling in classical cloud data centres is a well-studied topic in the literature, typically focusing on criteria such as maximising resource utilisation, minimising makespan, and balancing the load across computing resources [8]–[11]. However, quantum computing introduces additional critical considerations. In particular, remote gate operations

introduce infidelities that can adversely affect quantum computation tasks. These infidelities may arise from qubit decoherence during remote gate execution, as well as from imperfect remote entanglement generation between QPUs. Quantum-specific constraints, such as limited qubit coherence time, imply that circuit scheduling can directly impact not only execution time but also computational fidelity. Furthermore, prior studies [12] have shown that quantum circuits exhibit varying levels of sensitivity to errors arising from distributed execution. Therefore, a scheduling policy that accounts for these quantum-specific challenges can significantly enhance both system performance and overall computational fidelity.

Our main contributions are as follows:

- We address the problem of circuit scheduling in DQC interconnect networks, considering both traditional resource efficiency metrics and quantum-specific challenges such as fidelity degradation arising from remote operations.
- We consider a general heterogeneous network model that includes QPUs with varying capacities, arbitrary network topologies, and diverse types of QCircs.
- We propose two circuit scheduling algorithms that leverage both heuristic approaches and mixed-integer linear programming (MILP) formulations. The first method is based on dynamic batch scheduling, while the second adopts an online scheduling strategy.
- The proposed methods are extensively analysed and evaluated through detailed simulations.

A. Related work

In the literature, extensive research has focused on quantum compilation and circuit partitioning, with fewer efforts on execution management. Given the strong interdependencies among these tasks, we present key related works on these topics in what follows.

Several works have explored quantum compilation for DQC. Ferrari et al. [13] discussed challenges in compiler design for DQC and analytically characterised the overhead introduced by remote gates. Cuomo et al. [14] proposed compilation techniques to optimise circuit execution time and distributed entangled state usage. They modeled time as additional circuit depth layers due to entanglement generation, but their approach assumed uniform entanglement latency and neglected network topology. In a subsequent work, Ferrari et al. [15] presented a modular compilation framework incorporating network and QPU constraints. While this framework effectively considers network configuration and QPU characteristics, it primarily focuses on compilation and partitioning for a single circuit assigned to a fixed number of QPUs.

The problem of quantum circuit partitioning has been addressed in multiple research works. Daei et al. [16] represent QCircs as undirected graphs where qubits are nodes and edge weights correspond to the number of two-qubit gates shared between them. They then employ the Kernighan-Lin (K-L) algorithm to partition the graph, minimising the number of edges cut across partitions. In other studies [17]–[20], methods such as hypergraph partitioning, bipartite graph partitioning, and genetic algorithms have been employed to minimise the

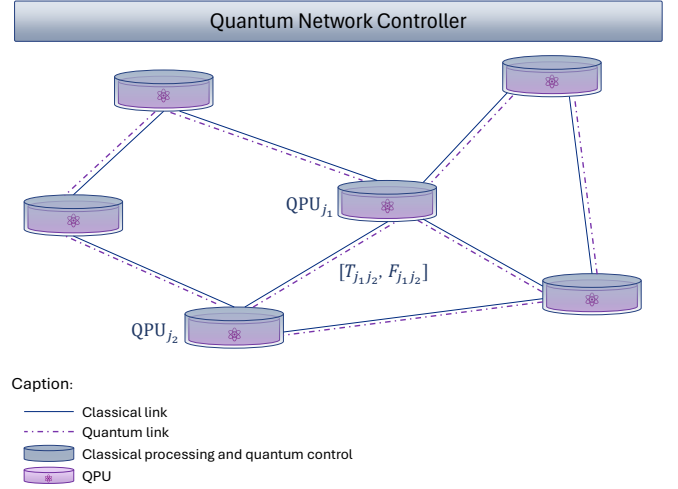


Fig. 3: A high-level abstract representation of the DQC network model.

number of remote gates. Andres et al. [21] extended previous works on circuit partitioning to the case of heterogeneous networks with arbitrary topologies. While these studies have focused on optimally partitioning a single QCirc assuming a fixed number of partitions, they have not explicitly considered the issue of resource competition when multiple QCircs are to be concurrently assigned.

Parekh et al. [22] proposed a resource allocation and scheduling algorithm based on a greedy approach that assigns QCircs and fills QPUs on a one-by-one basis. However, their algorithm does not take into account factors such as network topology and configuration, QPU decoherence properties, and the distinctive features of QCircs.

II. DQC NETWORK MODEL

We consider a DQC network in which QPUs are interconnected via both quantum and classical links. As discussed in [23], [24], promising architectures for quantum data centers may use optical switches to dynamically establish quantum links between QPUs. Techniques such as entanglement swapping and entanglement distillation can also be employed to generate high-fidelity entanglement between nodes. In this paper, to maintain generality, we adopt an abstract model that focuses on the logical topology of the network, without specifying the underlying physical architecture or hardware implementation.

As noted in the introduction, we assume that computational and network resource management are handled independently. Accordingly, our model focuses exclusively on computing qubits within QPUs, while communication qubits and their associated management are abstracted away.

A high-level representation of our DQC network model is shown in Fig. 3. In this abstract model, each quantum node is represented by QPU_j . A logical link between two QPUs, QPU_{j_1} and QPU_{j_2} , is characterised by two key parameters for remote gate execution: the remote gate execution time, denoted by T_{j_1,j_2} , and the fidelity of remote entanglement

generation, denoted by $F_{j_1 j_2}$. This model relies on several simplifying assumptions. First, we assume on-demand entanglement generation: remote entanglement generation is initiated and completed at the start of each remote gate operation, and the resulting entangled pair is used immediately. This eliminates the need for entangled-pair storage. Second, we assume fixed link parameters, meaning that both latency and fidelity values are constant for each logical link. This implicitly assumes a constant entanglement generation rate, as well as a fixed fidelity for remote entanglement generation between communication qubits.

We now turn to the key assumptions and definitions related to QPUs, the quantum nodes in our DQC network model. The set of QPUs in the network is denoted by $\mathcal{QP} = \{\text{QPU}_j\}_{j=1}^J$, where J represents the total number of QPUs in the network. The capacity of QPU_j , defined as its total number of computing qubits, is denoted by N_j . We also introduce a dynamic parameter n_j , which represents the current availability of QPU_j . Specifically, $n_j = N_j$ if QPU_j is available, and $n_j = 0$ otherwise. We assume that all QPUs are based on the same qubit technology and exhibit nearly identical decoherence properties, characterised by a common decoherence time parameter, T_{dec} . It is important to note that the specific interpretation of decoherence time can vary depending on the underlying quantum technology, such as trapped ions, superconducting qubits, and others. Nonetheless, for any given QPU technology, it is possible to identify a parameter that characterises the system's temporal limitations due to decoherence effects. To maintain platform independence, we abstract this aspect into a single representative parameter without loss of generality.

III. PROPOSED QCIRC SCHEDULING METHODS

In this section, we consider the problem of QCirc scheduling for the DQC network described above. The set of input quantum circuits to be scheduled and executed is denoted by $\mathcal{QC} = \{\text{QCirc}_m\}_{m=1}^M$, where M is the total number of circuits. Each circuit QCirc_m is characterised by three parameters:

- (a) the required number of qubits, denoted by w_m ;
- (b) the average number of two-qubit gates acting on each qubit, denoted by g_m ;
- (c) the standard deviation in the number of two-qubit gates per qubit, denoted by σ_m .

Let g_{mq_i} denote the number of two-qubit gates involving the i -th qubit in QCirc_m ; then g_m is defined as the average of g_{mq_i} over all qubits q_i , and σ_m is the corresponding standard deviation [25]:

$$g_m = \frac{1}{w_m} \sum_{i=1}^{w_m} g_{mq_i}, \quad \sigma_m = \sqrt{\frac{1}{w_m} \sum_{i=1}^{w_m} (g_{mq_i} - g_m)^2}.$$

Together, the parameters g_m and σ_m capture the internal connectivity and balance of the circuit, which are critical factors in distributed quantum computing.

In the following, we propose two primary QCirc scheduling methods. The first method, termed *Batch-QCirc Scheduling*, is based on dynamic batch scheduling, where a group of

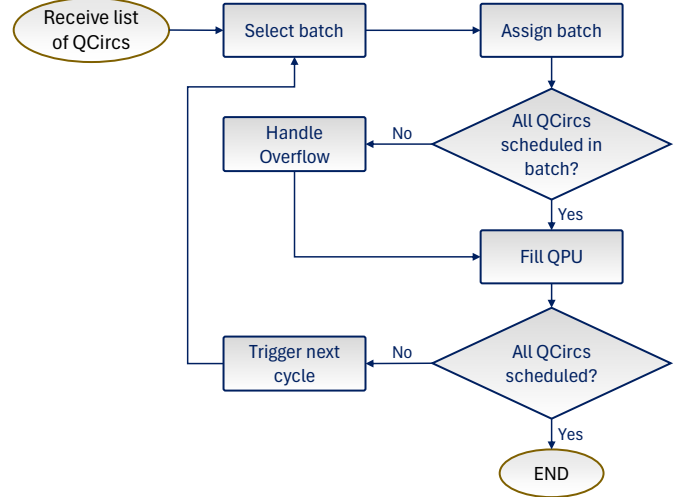


Fig. 4: Workflow of the Dynamic Batch-QCirc Scheduling Method.

circuits is selected and assigned to resources collectively. The second method, referred to as *Single-QCirc Scheduling*, assigns each circuit individually. Throughout this work, we assume a non-preemption model, meaning that once a QCirc begins execution on its allocated QPUs, it runs to completion without interruption.

A. Dynamic Batch-QCirc Scheduling

The workflow for the proposed batch scheduling method is illustrated in Fig. 4, and the corresponding algorithm pseudocode is outlined in Algorithm 1. In each scheduling cycle, a batch of circuits is selected from \mathcal{QC} . This batch is denoted by $\mathcal{B} = \{\text{QCirc}_m \mid m \in \mathcal{I}\}$, where $\mathcal{I} \subseteq \{1, \dots, M\}$ is the set of indices corresponding to the selected circuits. The batch size, $S = |\mathcal{I}|$, may vary across scheduling cycles.

We adopt a simple batch selection process, where elements of \mathcal{QC} are sequentially added to \mathcal{B} until the total required number of qubits, $c_{\text{req}} = \sum_{m \in \mathcal{I}} w_m$, exceeds a threshold βc_{tot} . Here, c_{tot} denotes the total qubit capacity of all available QPUs, given by $c_{\text{tot}} = \sum_j n_j$. The parameter β , fixed in the range $0 < \beta < 1$, is chosen to ensure that, with high probability, all circuits in the selected batch can be successfully assigned to available QPUs.

The selected batch then undergoes a batch assignment process, referred to as **ASSIGNBATCH** in Algorithm 1, where the circuits are mapped to the available QPUs. We have developed a heuristic batch assignment algorithm that leverages a MILP formulation, which will be described in detail in Sec. IV.

After the batch assignment, any circuits in the batch that remain unassigned are handled immediately using the **HANDLEOVERFLOW** procedure, described in Algorithm 2. The proposed overflow handling strategy is inspired by the scheduling method introduced in [8]. As shown in Algorithm 2, the circuits are first sorted according to their qubit requirements w_m , while the QPUs are sorted based on their expected busy time (EBT). The circuits are then assigned sequentially to the sorted QPUs, ensuring that they are served as soon

as resources become available. Notably, since β is selected to make overflow events rare, the overflow queue serves primarily as a failsafe rather than a central component of the workflow. Although our framework includes this mechanism for completeness, its use is expected to be minimal in practice.

To improve QPU utilisation, we incorporate a filling mechanism to address idle, unallocated QPUs. The FILLQPU algorithm, described in Algorithm 3, selects circuits from \mathcal{QC} and assigns each of them to idle QPUs individually, using a MILP-based optimisation strategy. To minimise the risk of excessive remote gate generation, only circuits with a ν_m value below a specified threshold are considered. The MILP-based Single QCirc assignment process (QCIRCASSIGN in Algorithm 3) will be described in detail in Sec. V.

Once all QPUs are allocated, the algorithm waits until a fraction α of the total qubit capacity across all QPUs, i.e., $\sum_j N_j$, becomes available, then proceeds to the next scheduling cycle. This mechanism is referred to as TRIGGERNEXTCYCLE in Algorithm 1.

Algorithm 1 Dynamic Batch-QCirc Scheduler

```

1: Input:  $\mathcal{QP}, \mathcal{QC}$ 
2: while not ISEMPTY( $\mathcal{QC}$ ) do
3:    $batch \leftarrow \text{SELECTBATCH}(\mathcal{QC}, \beta)$ 
4:    $batchMap \leftarrow \text{ASSIGNBATCH}(batch, \mathcal{QP})$ 
5:   if not ALLASSIGNED( $batch, batchMap$ ) then
6:      $\text{HANDLEOVERFLOW}(batch, batchmap, \mathcal{QP})$ 
7:   end if
8:    $\text{REMOVEASSIGNED}(\mathcal{QC}, batch)$ 
9:   if ANYAVAILABLE( $\mathcal{QP}$ ) then
10:     $\text{FILLQPU}(\mathcal{QC}, \mathcal{QP})$ 
11:   end if
12:    $\text{TRIGGERNEXTCYCLE}(\mathcal{QP}, \alpha)$ 
13: end while

```

Algorithm 2 HANDLEOVERFLOW

```

1: Input:  $batch, batchMap, \mathcal{QP}$ 
2: Sort unassigned QCircs in  $batch$  by decreasing  $w$ 
3: Sort QPUs in  $\mathcal{QP}$  by increasing EBT
4: for  $\text{QCirc}_m$  in sorted QCircs do
5:    $reqQubits \leftarrow w_m$ 
6:   while  $reqQubits \geq 0$  do
7:     Assign QCirc to next QPU from sorted  $\mathcal{QP}$ 
8:     Update  $reqQubits$ 
9:   end while
10: end for

```

B. Dynamic Single-QCirc Scheduling

Another approach for scheduling QCircs is to schedule them individually. To optimise this assignment, a MILP-based Single-QCirc assignment approach (Sec. V), similar to the one used in the Fill Algorithm (Algorithm 3), is employed.

IV. BATCH-QCIRC ASSIGNMENT

Batch-QCirc assignment refers to the mapping of a batch of QCircs to available QPUs within the dynamic batch-QCirc

Algorithm 3 FILLQPU

```

1: Input:  $\mathcal{QC}, \mathcal{QP}$ 
2:  $avlCapacity \leftarrow \sum_j N_j$  for idle QPUs
3: if  $avlCapacity > 0$  then
4:   for each  $\text{QCirc}_m$  in  $\mathcal{QC}$  do
5:     if  $\nu_m \leq \zeta$  and  $w_m \leq avlCapacity$  then
6:        $\text{ASSIGNQCIRC}(\text{QCirc}_m)$ 
7:        $\text{REMOVEASSIGNED}(\text{QCirc}_m)$ 
8:       Update  $avlCapacity$ 
9:     end if
10:   end for
11: end if

```

Algorithm 4 Single-QCirc Scheduler

```

1: Input:  $\mathcal{QC}, \mathcal{QP}$ 
2: while not ISEMPTY( $\mathcal{QC}$ ) do
3:   for each  $\text{QCirc}_m$  in  $\mathcal{QC}$  do
4:      $\text{ASSIGNQCIRC}(\text{QCirc}_m)$ 
5:      $\text{REMOVEASSIGNED}(\text{QCirc}_m)$ 
6:   end for
7: end while

```

scheduling framework. We propose an optimisation algorithm that improves this assignment by targeting three key objectives:

(a) Minimising decoherence-induced infidelity during remote gate executions across all QCircs: Remote gate operations typically incur significantly higher latency than local gates due to the need for both quantum and classical communication across QPUs. This increased latency exposes the computing qubits assigned to the QCircs to greater decoherence. When remote gates are invoked repeatedly within a QCirc, the cumulative effect can result in substantial fidelity loss, thereby degrading the accuracy of distributed quantum computations. Minimising this detrimental impact, considering the effects across the entire batch of QCircs, is therefore one of our primary objectives.

(b) Minimising infidelity from remote entanglement generation: Remote entanglement generation is typically imperfect, introducing some level of infidelity during its implementation. This fidelity can be further altered through operations such as entanglement swapping and entanglement distillation. As discussed in Section 2, we adopt an abstract network model in this paper, where each inter-QPU link is characterised by a fixed infidelity parameter, without delving into the specifics of the underlying physical infrastructure. Similar to the decoherence effects discussed earlier, repeated use of remote gates within a QCirc leads to cumulative fidelity degradation. Our objective is to mitigate this degradation, taking into account the fidelity impact across the entire batch of QCircs.

(c) Maximising the number of assigned QCircs: This objective is primarily aimed at enhancing system throughput and optimising resource utilisation.

The output of the Batch-QCirc assignment process comprises three key components: (a) the partition number assigned to each QCirc, (b) the specific QPUs allocated to each QCirc,

and (c) the number of QPU qubits allocated to each circuit partition. This information is subsequently used by the circuit partitioning algorithm to efficiently decompose each QCirc into smaller sub-circuits.

A. Problem Formulation

To mathematically formulate the problem of batch-QCirc assignment, we begin by defining the following variables, which represent the outputs we aim to determine:

- Let x_{mj} be a binary variable representing the number of qubits from QCirc_m that are assigned to QPU_j .
- Let r_{mj} be a binary variable, where $r_{mj} = 1$ if $x_{mj} > 0$, and $r_{mj} = 0$ otherwise.
- Let b_m be a binary variable, where $b_m = 1$ if QCirc_m is successfully assigned, i.e., $\sum_j r_{mj} > 0$, and $b_m = 0$ otherwise.

In the following subsections, we formulate the objective functions and constraints to establish our multi-objective optimisation problem.

1) *Objective 1: minimising decoherence-induced infidelity:* We define a cost function that captures the degrading impact of qubit decoherence during remote gate executions, as follows:

$$C_{\text{dec}} = \left(\frac{1}{T_{\text{dec}}}\right) \sum_m \sum_{j_1} \sum_{j_2 > j_1} \nu_m w_m r_{mj_1} r_{mj_2} T_{j_1 j_2}, \quad (1)$$

where $T_{j_1 j_2}$ represents the latency parameter associated with a remote gate involving QPU_{j_1} and QPU_{j_2} . The term $T_{j_1 j_2}/T_{\text{dec}}$ captures the relative decoherence impact of a single remote gate execution. To account for circuit-specific features, we incorporate several weighting factors into the cost function. The qubit count w_m reflects the potential exposure of circuit QCirc_m to decoherence. The parameter ν_m , defined as

$$\nu_m = \lambda g_m + (1 - \lambda) \sigma_m, \quad 0 < \lambda < 1,$$

effectively captures the internal connectivity pattern of QCirc_m , which is highly correlated with the probability of generating remote gates after partitioning. Since the exact number of remote gates per circuit is unknown until after circuit partitioning (which follows batch assignment), we incorporate ν_m into the cost function to represent the circuit's potential for remote gate generation. This surrogate cost term enables the heuristic optimisation algorithm to make informed scheduling decisions while maintaining computational tractability.

2) *Objective 2: minimising infidelity from remote entanglement generation:* The second objective is defined as follows:

$$C_{\text{reg}} = \sum_m \sum_{j_1} \sum_{j_2 > j_1} \nu_m r_{mj_1} r_{mj_2} (1 - F_{j_1 j_2}). \quad (2)$$

Here, $F_{j_1 j_2}$ represents the fidelity parameter associated with remote entanglement generation between QPU_{j_1} and QPU_{j_2} . Similar to Objective 1, the parameter ν_m is incorporated to account for the circuit's connectivity pattern and its tendency to produce remote gates.

3) *Objective 3: maximising the number of assigned QCircs:* The objective of maximising successfully assigned QCircs can be formulated as:

$$C_{\text{asg}} = - \sum_{m=1}^M b_m \quad (3)$$

The negative sign converts the maximisation of assigned QCircs into an equivalent minimisation goal.

4) *Multi-objective Optimisation problem:* Our multi-objective optimisation is shown in **Problem Formulation 1**. Four primary constraints are considered and mathematically represented within this formulation. Their corresponding explanations are provided below.

- Each quantum circuit, QCirc_m , must be either fully assigned or left entirely unassigned.
- Circuit partitions cannot exceed the qubit capacity of their allocated QPUs.
- The number of partitions for the quantum circuit QCirc_m is restricted to be less than or equal to K_m^{max} , a predefined threshold. This threshold can be specified by the user or the network controller based on various factors, such as quantum data centre policies, circuit size, and error tolerance.
- Only a single circuit partition is assigned to a QPU.

B. MILP-based optimisation method

To formulate our optimisation problem as a MILP, we first linearise the non-linear terms by introducing an auxiliary binary variable [26]:

$$z_{mj_1 j_2} = r_{mj_1} r_{mj_2}. \quad (4)$$

and the following constraints:

$$r_{mj_1} + r_{mj_2} - 1 \leq z_{mj_1 j_2} \leq \min(r_{mj_1}, r_{mj_2}) \quad (5)$$

With this linearisation, the problem can be reformulated as a MILP, as outlined in **Problem Formulation 2**. The parameter γ is a fixed constant larger than $\max\{N_j\}$.

To address the multi-objective nature of the problem, we employ the ε -constraint method [27], which converts the problem into a single-objective formulation. Specifically, we minimise C_{dec} while imposing constraints on C_{reg} and C_{asg} .

V. SINGLE-QCIRC ASSIGNMENT

Single-QCirc assignment focuses on optimally mapping a single QCirc to the available QPUs. To this end, we adapt the MILP formulation introduced in the previous section, simplifying it for the single-circuit case. The resulting MILP formulation is presented in **Problem Formulation 3**.

VI. EVALUATION AND RESULTS

This section evaluates the proposed scheduling algorithms through simulations. We consider a DQC network consisting of 16 QPUs within a data center. The QPUs have the following capacities: four QPUs with capacity 8, four with capacity 12, four with capacity 16, and four with capacity 20. These capacities are randomly assigned to QPUs using a fixed

$$\begin{aligned}
& \min \{C_{\text{dec}}, C_{\text{reg}}, C_{\text{asg}}\} \\
& \text{s.t.} \\
& \sum_{j=1}^J x_{mj} = b_m w_m \quad \text{for } m = 1, \dots, M \\
& \sum_{m=1}^M x_{mj} \leq n_j \quad \text{for } j = 1, \dots, J \\
& \sum_{j=1}^J r_{mj} \leq K_m^{\max} \quad \text{for } m = 1, \dots, M \\
& \sum_{m=1}^M r_{mj} \leq 1 \quad \text{for } j = 1, \dots, J
\end{aligned}$$

Problem Formulation 1: Batch-QCirc assignment problem formulation.

$$\begin{aligned}
& \min \left(\frac{1}{T_{\text{dec}}} \right) \sum_m \sum_{j_1} \sum_{j_2 > j_1} \nu_m w_m z_{mj_1 j_2} T_{j_1 j_2} \\
& \text{s.t.} \\
& \sum_m \sum_{j_1} \sum_{j_2 > j_1} \nu_m z_{mj_1 j_2} (1 - F_{j_1 j_2}) \leq th \\
& - \sum_{m=1}^M b_m \leq \kappa \\
& \sum_{j=1}^J x_{mj} = b_m w_m \quad \text{for } m = 1, \dots, M \\
& \sum_{m=1}^M x_{mj} \leq n_j \quad \text{for } j = 1, \dots, J \\
& \sum_{j=1}^J r_{mj} \leq K_m^{\max} \quad \text{for } m = 1, \dots, M \\
& \sum_{m=1}^M r_{mj} \leq 1 \quad \text{for } j = 1, \dots, J \\
& r_{mj} \leq x_{mj} \leq \gamma r_{mj} \quad \text{for } m = 1, \dots, M \quad j = 1, \dots, J \\
& b_m \leq \sum_{j=1}^J r_{mj} \leq \gamma b_m \quad \text{for } m = 1, \dots, M \\
& z_{mj_1 j_2} \leq r_{mj_1} \quad \text{for } m = 1, \dots, M \quad j_1, j_2 = 1, \dots, J \quad j_2 > j_1 \\
& z_{mj_1 j_2} \leq r_{mj_2} \quad \text{for } m = 1, \dots, M \quad j_1, j_2 = 1, \dots, J \quad j_2 > j_1 \\
& z_{mj_1 j_2} \geq r_{mj_1} + r_{mj_2} - 1 \quad \text{for } m = 1, \dots, M \\
& \quad \quad \quad j_1, j_2 = 1, \dots, J \quad j_2 > j_1
\end{aligned}$$

Problem Formulation 2: MILP-based Batch-QCirc assignment problem formulation.

TABLE I: List of key notations and parameters

Paramter	Definition
\mathcal{QP}	Set of all QPUs
\mathcal{QC}	Set of all QCircs
\mathcal{B}	Selected batch of QCircs
J	Number of QPUs
M	Number of QCircs
S	Number of QCircs in the selected batch
T_{dec}	Decoherence time parameter of QPUs
N_j	Number of computing qubits within QPU _{<i>j</i>}
n_j	Equals to N_j if QPU _{<i>j</i>} is available, and 0 otherwise
w_m	Number of qubits required for QCirc _{<i>m</i>}
ν_m	Average number of two-qubit gates acting on each qubit in QCirc _{<i>m</i>}
x_{mj}	Number of computing qubits within QPU _{<i>j</i>} assigned to QCirc _{<i>m</i>}
r_{mj}	Equals to 1 if $x_{mj} > 0$, and 0 otherwise
b_m	Equals to 1 if QCirc _{<i>m</i>} is assigned, and 0 otherwise
$T_{j_1 j_2}$	The latency parameter associated with remote gate execution, involving QPU _{<i>j_1</i>} and QPU _{<i>j_2</i>}
$F_{j_1 j_2}$	The fidelity parameter associated with remote remote entanglement generation between QPU _{<i>j_1</i>} and QPU _{<i>j_2</i>}

$$\min \left(\frac{1}{T_{\text{dec}}} \right) \sum_{j_1} \sum_{j_2 > j_1} z_{mj_1 j_2} T_{j_1 j_2}$$

s.t.

$$\sum_{j_1} \sum_{j_2 > j_1} z_{mj_1 j_2} (1 - F_{j_1 j_2}) \leq th$$

$$\sum_{j=1}^J x_{mj} = w_m$$

$$x_{mj} \leq n_j \quad \text{for } j = 1, \dots, J$$

$$\sum_{j=1}^J r_{mj} \leq K_m^{\max}$$

$$r_{mj} \leq x_{mj} \leq \gamma r_{mj} \quad \text{for } j = 1, \dots, J$$

$$z_{mj_1 j_2} \leq r_{mj_1} \quad \text{for } j_1, j_2 = 1, \dots, J \quad j_2 > j_1$$

$$z_{mj_1 j_2} \leq r_{mj_2} \quad \text{for } j_1, j_2 = 1, \dots, J \quad j_2 > j_1$$

$$z_{mj_1 j_2} \geq r_{mj_1} + r_{mj_2} - 1 \quad \text{for } j_1, j_2 = 1, \dots, J \quad j_2 > j_1$$

Problem Formulation 3: MILP-based Single-QCirc assignment problem formulation.

random seed to ensure consistent QPU configurations across all simulations. The entire simulation process is repeated for 10 different seed values, and the average results are presented.

The network adopts a 4-pod fat-tree topology [28], as illustrated in Fig. 5. In Sec. II, we defined two key parameters characterising the links in the logical topology: latency ($T_{j_1 j_2}$) and fidelity ($F_{j_1 j_2}$). Here, we specify their values for the 4-pod fat-tree topology used in our simulations. This topology features three types of links, distinguished by the number of optical switches along the path—specifically, 1, 3, or 5 switches. We denote the corresponding latency values by T_{link_1} , T_{link_3} , and T_{link_5} , respectively. Assuming an elementary link latency of T_{el} (corresponding to a link without any optical switches), and noting that the entanglement generation rate is directly affected by link loss, the latency for each link type is

calculated using the formula:

$$T_{\text{link}_{n_s}} = \frac{T_{\text{el}}}{\eta_s^{n_s}},$$

where η_s is the switch transmission efficiency and $n_s \in \{1, 3, 5\}$ is the number of switches in the path. In our simulations, we assume that all optical switches are of the same type and have an identical loss of 0.5 dB. Given the short physical distances between QPUs in a data center environment, propagation delays are considered negligible. For the fidelity parameter, we assume an identical value across all links.

To establish the set of quantum circuits, QC , benchmark circuits from the Munich toolkit [29] are used. The simulation considers a pool of four distinct QCirc types: Quantum Fourier Transform (QFT), Deutsch-Jozsa (DJ), WState, and GHZ state. QCircs are randomly selected from this pool, with the number of qubits w_m for each circuit sampled from a range \mathcal{R}_w . Two cases are studied: (a) $\mathcal{R}_w = [20, 30]$ and $\mathcal{R}_w = [30, 40]$. In both cases, the value of w_m is reduced by 10 whenever a QFT circuit is selected—that is, a reduced range is effectively used for QFT—to account for the faster scaling of ν_m with w_m . As before, simulations are repeated across 10 fixed random seeds, and the results are averaged.

To solve the MILP optimisation problems presented in Problem Formulations 2 and 3, the Python-MIP package with the Gurobi optimiser is used. The threshold for C_{asg} , denoted as κ , is initially set to M , and it is decremented until a valid solution is found. Once the optimal assignment is obtained, we proceed to partition each quantum circuit individually using the Kernighan-Lin algorithm provided by the NetworkX library. This algorithm determines both the number of remote gates between QPU pairs and the total number of remote gates for each QCirc. For circuits requiring partitioning into more than two parts, the Kernighan-Lin algorithm is applied iteratively until the desired number of partitions is achieved.

To evaluate the performance of the proposed scheduling methods, we consider several key figures of merit. All results are averaged over repeated simulation runs.

- **Number of remote gates per QCirc:** the total number of remote gates across all M QCircs, divided by M .
- **Number of circuit partitions per QCirc:** the total number of circuit partitions across all M QCircs, divided by M .
- **Normalised Job Execution Time (JET)** for each QCirc type: Average execution time for each QCirc type, normalised by T_{dec} , i.e., $\text{JET}/T_{\text{dec}}$.
- **Normalised Makespan:** the total time required to complete all jobs (i.e., the execution of all M QCircs), normalised by T_{dec} , for consistency with normalised JET and to ensure hardware platform independence.
- **Normalised Throughput:** defined as the ratio of the number of QCircs, M , to Normalised Makespan.
- **QPU usage**, defined as follows:

$$\text{QPU Usage} = \frac{\sum_j N_j \times \text{TBT}(\text{QPU}_j)}{(\sum_j N_j)(\text{Makespan})} \quad (6)$$

Here, “TBT” is Total Busy Time for a QPU. As a baseline, random scheduling is used for comparison.

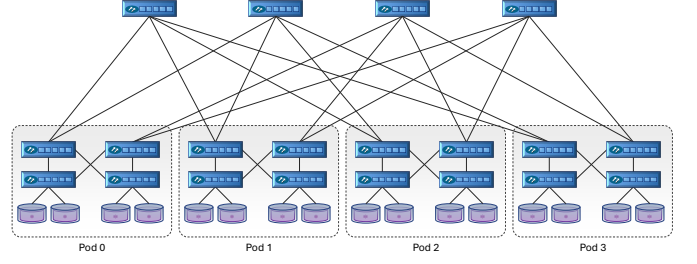


Figure 5: A 16-QPU DQC network with 4-pod fat-tree topology.

The normalised JET for a specific QCirc is obtained under the following assumptions. First, we assume that remote gates within a layer of a given QCirc are executed sequentially rather than in parallel, in accordance with current and near-future technological limitations. Second, we assume that all local gates have identical execution durations. Based on these assumptions, we iterate through all circuit layers and identify whether each layer contains any remote gates or only local gates. Let N_{LL} denote the number of layers containing only local gates. We compute the normalised JET using the following expression:

$$\frac{\text{JET}}{T_{\text{dec}}} = N_{\text{LL}} \frac{T_{\text{local}}}{T_{\text{dec}}} + \sum_{n_s \in \{1, 3, 5\}} N_{\text{link}_{n_s}}^{(rg)} \frac{T_{\text{link}_{n_s}}}{T_{\text{dec}}} \quad (7)$$

where $N_{\text{link}_{n_s}}^{(rg)}$ denotes the number of remote gates in the QCirc under consideration that are executed across the links with n_s optical switches. In all simulations and calculations, we assume $T_{\text{local}}/T_{\text{dec}} = 5 \times 10^{-4}$ and $T_{\text{el}}/T_{\text{dec}} = 0.005$.

Figure 6 presents the average remote gate count and partition count per QCirc for the proposed scheduling methods, compared against random scheduling as a baseline. For the batch-QCirc assignment method, several values of the parameter α are considered. As shown, both the batch-QCirc and single-QCirc methods yield significant improvements in these metrics. Moreover, in all cases, the batch-QCirc method outperforms the single-QCirc approach. These results are particularly important, as the number of remote gates directly reflects the demand for communication resources. Therefore, the findings demonstrate that both proposed methods—and especially the batch-QCirc assignment—effectively reduce communication overhead.

Next, we evaluate the normalised Job Execution Time (JET) across all circuit types. As shown in Fig. 7, the proposed methods generally outperform the baseline. Specifically, for the qubit range $\mathcal{R}_w = [20, 30]$, the JET is reduced in almost all cases, with batch-QCirc scheduling outperforming the single-QCirc approach.

For $\mathcal{R}_w = [30, 40]$, the results vary by circuit type. For QFT and DJ circuits, batch-QCirc scheduling achieves the lowest JET, while single-QCirc still performs better than random scheduling. In contrast, for W-state and GHZ circuits, the best-performing method depends on both the circuit type and the value of M . For example, in the case of GHZ circuits, the

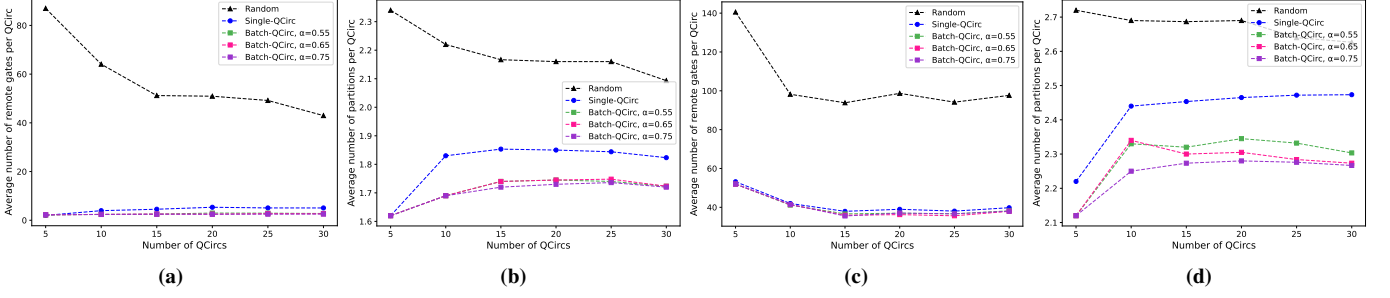


Figure 6: Average number of remote gates and circuit partitions per QCirc for the proposed and baseline scheduling methods. For the batch-QCirc approach, several values of the parameter α are considered. (a)–(b): $\mathcal{R}_w = [20, 30]$, (c)–(d): $\mathcal{R}_w = [30, 40]$.

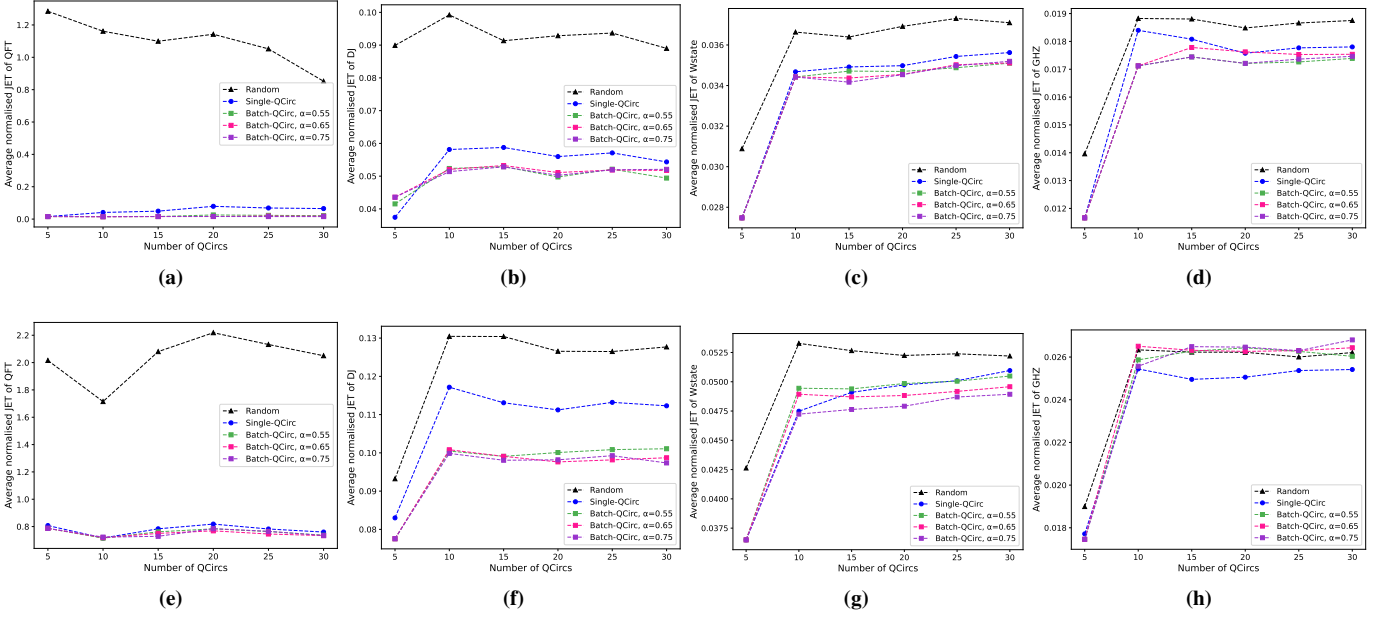


Figure 7: Average Job Execution Time (JET), normalised by T_{dec} , for the proposed and baseline scheduling methods across different circuit types. (a)–(d): $\mathcal{R}_w = [20, 30]$; (e)–(h): $\mathcal{R}_w = [30, 40]$.

single-QCirc scheduler achieves the lowest JET in nearly all cases, except when $M = 5$.

It is also worth noting that the normalised JET values for QFT circuits are higher overall compared to GHZ circuits, which aligns with their corresponding ν_m values. These results highlight the system-level, holistic nature of resource management in batch-QCirc scheduling, where trade-offs may arise—for instance, reducing the JET of highly connected circuits at the expense of not fully optimising the JET of circuits with lower connectivity.

Overall, these results demonstrate the effectiveness of the proposed methods in reducing the JET of quantum circuits. This improvement is particularly significant for circuits with higher ν_m values, such as the QFT circuits in our simulations. It can be observed that under random scheduling, the normalised JET (i.e., $\text{JET}/T_{\text{dec}}$) often exceeds 1, which may render successful execution infeasible due to decoherence. However, by applying the proposed methods, this ratio is significantly reduced, enabling more reliable circuit execution within the coherence time constraints.

Next, we examine the normalised makespan, normalised throughput, and QPU usage. The results are shown in Fig. 8. Compared to random scheduling, the proposed methods significantly improve all three metrics in nearly all cases. Additionally, the batch-QCirc approach outperforms the single-QCirc variant in most scenarios, especially when $\mathcal{R} = [20, 30]$. These improvements are primarily driven by the reduction in JET.

It is important to note that QPU usage alone is not a sufficient indicator of resource efficiency; it should be interpreted alongside the makespan to enable a proper evaluation of scheduling performance.

Lastly, we compare the results for batch-QCirc scheduling with varying values of α , as presented across Figures 6, 7, and 8. In terms of makespan, throughput, and QPU usage, $\alpha = 0.75$ consistently yields the worst performance, whereas $\alpha = 0.55$ or $\alpha = 0.65$ typically perform best. Since the parameter α determines when the algorithm proceeds to the next scheduling cycle, it plays a crucial role in these metrics. Looking at the results for remote gate count and JET, $\alpha = 0.75$ does not show meaningful improvements over $\alpha = 0.55$ or $\alpha = 0.65$; in fact,

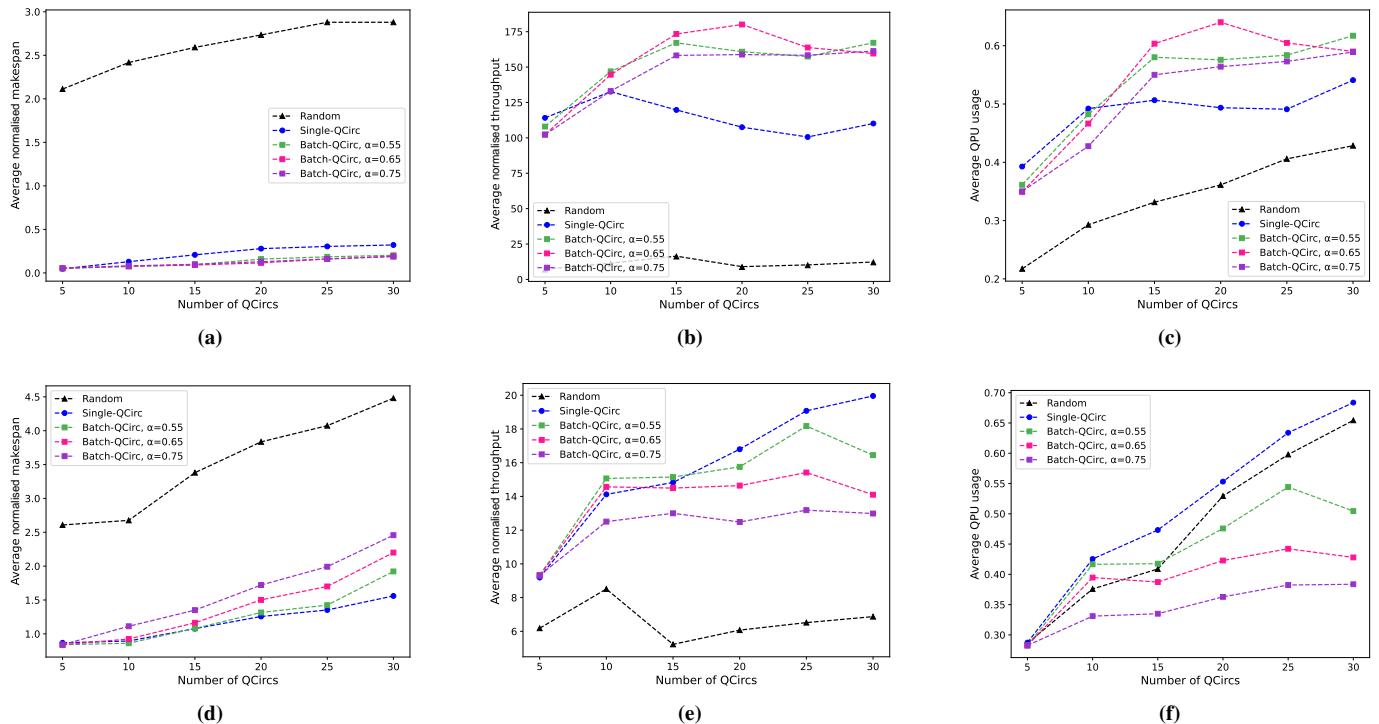


Figure 8: Average Makespan, Throughput, and QPU Usage for the proposed and baseline scheduling methods. Makespan and, by extension, Throughput are normalised by T_{dec} . (a)–(c): $\mathcal{R}_w = [20, 30]$; (d)–(f): $\mathcal{R}_w = [30, 40]$.

the latter two often outperform it. These findings indicate that increasing α too much can lead to unnecessary resource waste without performance gains.

VII. CONCLUSION

In this work, we addressed the challenge of efficient resource management and QCirc scheduling in distributed quantum computing (DQC) networks, with a particular focus on computing resources. We proposed two scheduling approaches: a dynamic batch-QCirc scheduling method, which operates through sequential scheduling cycles with batch optimisation, and a single-QCirc scheduling method that optimises QCirc allocation individually.

To achieve optimal assignment of QCircs to QPUs, we developed MILP formulations that jointly consider multiple objectives, including minimising inter-QPU infidelities and maximising QCirc throughput. These formulations also account for network topology, link latencies, QPU capacities, and QCirc structure, enabling effective and quantum-aware resource assignment. We evaluated both approaches through extensive simulations, showing that our methods support reliable QCirc execution while improving overall resource utilisation.

This work marks an initial step toward quantum-aware and network-aware job scheduling in cloud-based quantum data centres, incorporating key quantum-specific features such as qubit decoherence, as well as network-level considerations like topology. Several directions remain open for future research. First, our current model does not incorporate job priorities or deadlines. Future studies could develop more

advanced scheduling strategies that address these aspects. Additionally, a detailed queue analysis under realistic quantum traffic models could provide deeper insights. Finally, leveraging machine learning techniques—particularly reinforcement learning—may enable the development of adaptive, scalable scheduling algorithms suited to complex quantum workloads.

This work provides a stepping stone toward scalable and intelligent resource management in future quantum cloud infrastructures.

ACKNOWLEDGMENT

This work was supported by the Quantum Communication Hub funded by the EPSRC grant ref. EP/T001011/1 and the Quantum Data Centre of Future UKRI project (10004793). The authors would like to express their sincere gratitude to Prof. Reza Nejabati for his support and insightful technical discussions.

REFERENCES

- [1] A. Yimsiriwattana and S. J. Lomonaco Jr, “Distributed quantum computing: A distributed shor algorithm,” in *Quantum Information and Computation II*, vol. 5436. SPIE, 2004, pp. 360–372.
- [2] D. Cuomo, M. Caleffi, and A. S. Cacciapuoti, “Towards a distributed quantum computing ecosystem,” *IET Quantum Communication*, vol. 1, no. 1, pp. 3–8, 2020.
- [3] M. Caleffi *et al.*, “Distributed quantum computing: a survey,” *arXiv preprint arXiv:2212.10609*, 2022.
- [4] J. Ang *et al.*, “Architectures for multinode superconducting quantum computers,” *arXiv preprint arXiv:2212.06167*, 2022.
- [5] Y. Shi, P. Gokhale, P. Murali, J. M. Baker, C. Duckering, Y. Ding, N. C. Brown, C. Chamberland, A. Javadi-Abhari, A. W. Cross *et al.*, “Resource-efficient quantum computing by breaking abstractions,” *Proceedings of the IEEE*, vol. 108, no. 8, pp. 1353–1370, 2020.

- [6] K. Campbell, A. Lawey, and M. Razavi, "Quantum data centres: a simulation-based comparative noise analysis," *Quantum Science and Technology*, vol. 10, no. 1, p. 015052, 2024.
- [7] M. Maronese, L. Moro, L. Rocutto, and E. Prati, "Quantum compiling," in *Quantum Computing Environments*. Springer, 2022, pp. 39–74.
- [8] A. Hussain, M. Aleem, A. Khan, M. A. Iqbal, and M. A. Islam, "Ralba: a computation-aware load balancing scheduler for cloud computing," *Cluster Computing*, vol. 21, pp. 1667–1680, 2018.
- [9] S. Singhal and A. Sharma, "Resource scheduling algorithms in cloud computing: A big picture," in *2021 5th International Conference on Information Systems and Computer Networks (ISCON)*. IEEE, 2021, pp. 1–6.
- [10] S. K. Mishra, B. Sahoo, and P. P. Parida, "Load balancing in cloud computing: a big picture," *Journal of King Saud University-Computer and Information Sciences*, vol. 32, no. 2, pp. 149–158, 2020.
- [11] O. Elzeki, M. Rashad, and M. A. Elsoud, "Overview of scheduling tasks in distributed computing systems," *International Journal of Soft Computing and Engineering*, vol. 2, no. 3, pp. 470–475, 2012.
- [12] R. D. Oliveira, S. Bahrani, E. Arabul, R. Wang, R. Nejabati, and D. Simeonidou, "FPGA-based deterministic and low-latency control for distributed quantum computing," in *IEEE INFOCOM 2023-IEEE Conference on Computer Communications Workshops (INFOCOM WK-SHPS)*. IEEE, 2023, pp. 1–6.
- [13] D. Ferrari, A. S. Cacciapuoti, M. Amoretti, and M. Caleffi, "Compiler design for distributed quantum computing," *IEEE Transactions on Quantum Engineering*, vol. 2, pp. 1–20, 2021.
- [14] D. Cuomo, M. Caleffi, K. Krsulich, F. Tramonto, G. Agliardi, E. Prati, and A. S. Cacciapuoti, "Optimized compiler for distributed quantum computing," *ACM Transactions on Quantum Computing*, vol. 4, no. 2, pp. 1–29, 2023.
- [15] D. Ferrari, S. Carretta, and M. Amoretti, "A modular quantum compilation framework for distributed quantum computing," *IEEE Transactions on Quantum Engineering*, 2023.
- [16] O. Daei *et al.*, "Optimized quantum circuit partitioning," *International Journal of Theoretical Physics*, vol. 59, no. 12, pp. 3804–3820, 2020.
- [17] W. Cambiucci *et al.*, "Hypergraphic partitioning of quantum circuits for distributed quantum computing," *arXiv preprint arXiv:2301.05759*, 2023.
- [18] P. Andres-Martinez *et al.*, "Automated distribution of quantum circuits via hypergraph partitioning," *Physical Review A*, vol. 100, no. 3, p. 032308, 2019.
- [19] Z. Davarzani, M. Zomorodi-Moghadam, M. Houshmand, and M. Nouri-Baygi, "A dynamic programming approach for distributing quantum circuits by bipartite graphs," *Quantum Information Processing*, vol. 19, pp. 1–18, 2020.
- [20] D. Dadkhah, M. Zomorodi, and S. E. Hosseini, "A new approach for optimization of distributed quantum circuits," *International Journal of Theoretical Physics*, vol. 60, pp. 3271–3285, 2021.
- [21] P. Andres-Martinez, T. Forrer, D. Mills, J.-Y. Wu, L. Henaut, K. Yamamoto, M. Murao, and R. Duncan, "Distributing circuits over heterogeneous, modular quantum computing network architectures," *arXiv preprint arXiv:2305.14148*, 2023.
- [22] R. Parekh *et al.*, "Quantum algorithms and simulation for parallel and distributed quantum computing" in *2021 IEEE/ACM Second International Workshop on Quantum Computing Software (QCS)*. IEEE, 2021, pp. 9–19.
- [23] H. Shapourian *et al.*, "Quantum data center infrastructures: A scalable architectural design perspective," *arXiv preprint arXiv:2501.05598*, 2025.
- [24] J. Ang, G. Carini, Y. Chen, I. Chuang, M. Demarco, S. Economou, A. Eickbusch, A. Faraon, K.-M. Fu, S. Girvin *et al.*, "Arquin: architectures for multinode superconducting quantum computers," *ACM Transactions on Quantum Computing*, vol. 5, no. 3, pp. 1–59, 2024.
- [25] A. Li, S. Stein, S. Krishnamoorthy, and J. Ang, "Qasmbench: A low-level quantum benchmark suite for nisq evaluation and simulation," *ACM Transactions on Quantum Computing*, vol. 4, no. 2, pp. 1–26, 2023.
- [26] P. Belotti, C. Kirches, S. Leyffer, J. Linderoth, J. Luedtke, and A. Mahajan, "Mixed-integer nonlinear optimization," *Acta Numerica*, vol. 22, pp. 1–131, 2013.
- [27] Y. Haimes, "On a bicriterion formulation of the problems of integrated system identification and system optimization," *IEEE transactions on systems, man, and cybernetics*, no. 3, pp. 296–297, 1971.
- [28] C. E. Leiserson, "Fat-trees: Universal networks for hardware-efficient supercomputing," *IEEE transactions on Computers*, vol. 100, no. 10, pp. 892–901, 1985.
- [29] <https://www.cda.cit.tum.de/mqtbench/>.